

Winning Ticket in Noisy Image Classification

Taehyeon Kim^{*1} Jongwoo Ko^{*1} Jinhwan Choi¹ Sangwook Cho¹ Seyoung Yun¹

Abstract

Modern deep neural networks (DNNs) become frail when the datasets contain noisy (incorrect) class labels. Many robust techniques have emerged via loss adjustment, robust loss function, and clean sample selection to mitigate this issue using the whole dataset. Here, we empirically observe that the dataset which contains only clean instances in original noisy datasets leads to better optima than the original dataset even with fewer data. Based on these results, we state the *winning ticket hypothesis*: regardless of robust methods, any DNNs reach the best performance when trained on the dataset possessing only clean samples from the original (*winning ticket*). We propose two simple yet effective strategies to identify winning tickets by looking at the loss landscape and latent features in DNNs. We conduct numerical experiments by collaborating the two proposed methods purifying data and existing robust methods for CIFAR-10 and CIFAR-100. The results support that our framework consistently and remarkably improves the performance.

1. Introduction

Deep neural networks have achieved remarkable success in numerous tasks as the number of accessible data dramatically increases (Krizhevsky et al., 2012; He et al., 2016). On the other side, these datasets have been labeled through a labor-intensive job with human or web crawling (Yu et al., 2018) so that they may be easily corrupted (*label noise*). It is well-known that even a small number of noisy samples can severely cause performance degradation issues (Zhang et al., 2016).

One possible approach to handling the noisy samples is to filter the *clean data* (i.e., samples with uncorrupted labels)

^{*}Equal contribution ¹Graduate School of AI, KAIST, Daejeon, Republic of Korea. Correspondence to: Taehyeon Kim <potter32@kaist.ac.kr>, Jongwoo Ko <jongwoo.ko@kaist.ac.kr>, Jinhwan Choi <jinhwanchoi@kaist.ac.kr>, Sangwook Cho <sangwookcho@kaist.ac.kr>, Seyoung Yun <yunseyoung@kaist.ac.kr>.

Preliminary work.

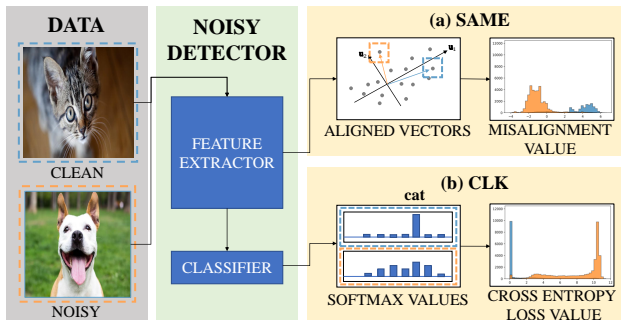


Figure 1. An illustration of strategies to identify the winning ticket; we propose two strategies (a) **SAME** uses a feature extractor as a **NOISYDETECTOR** to measure the misalignment of pre-logits. (b) **CLK** uses a classifier as a **NOISYDETECTOR** to cluster by utilizing the k-means algorithm based on cross-entropy loss values between the prediction and labeled one-hot vector.

from the original dataset (Jiang et al., 2018; Han et al., 2018; Yu et al., 2019; Wu et al., 2020). Most filtering methods perform a dynamical segregation process per every training iteration to resist label corruption. They generally assumed that the noisy data might have a large loss (Jiang et al., 2018; Han et al., 2018; Yu et al., 2019) or magnitude of the gradient during training (Zhang & Sabuncu, 2018; Wang et al., 2019b), but these heuristics lack theoretical supports for any noise patterns. Recently, in (Wu et al., 2020), the authors considered the topological properties of the data in latent space during training, but it is computationally expensive and hard to tune due to its additional learnable parameters and hyperparameters (Shu et al., 2020). The latent representations might have imperfect information to predict the sample correctly in the training dynamics. We rearticulate these studies as the *winning ticket hypothesis*.

Winning Ticket Hypothesis (WTH) *Any neural network trained on the dataset possessing the bundle of clean samples from the original dataset has better performance than the network trained on the original dataset, even when such a subset has significantly a fewer number of data than the original dataset.*

To deal with the noisy samples, this paper proposes a train-filter-train training flow (TFT) that first trains a proxy model with the whole data, finds the winning ticket with posterior information from the proxy model, and finally trains the target model on the distilled dataset. Unlike the previous

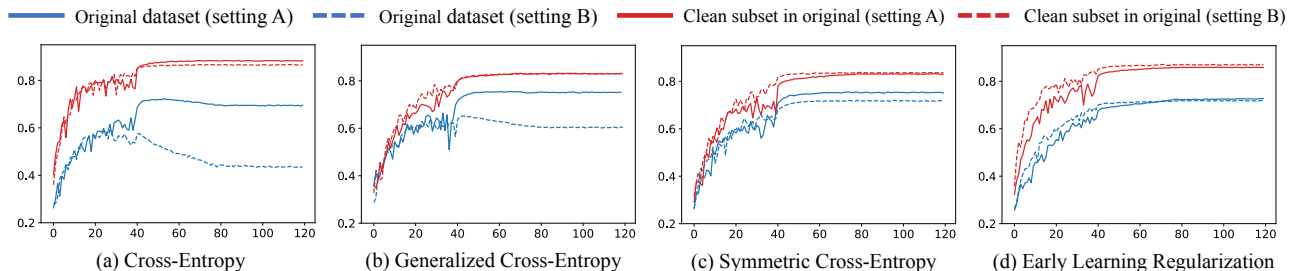


Figure 2. Test accuracies of the ResNet34 models on noisy labels trained with robust loss function methods such as cross-entropy loss (CE), generalized cross-entropy (GCE) (Zhang & Sabuncu, 2018), symmetric cross-entropy (SCE) (Wang et al., 2019b), and early learning regularization (ELR) (Liu et al., 2020). Blue and red lines indicate the learning curve on the whole noisy data and the entire clean data from the former noisy dataset, respectively. Solid lines indicate the learning curve with optimal hyperparameter settings mentioned in (Liu et al., 2020), and dotted lines indicate the learning curve with other popular settings in (Zhang & Sabuncu, 2018).

sample-selection methods (Malach & Shalev-Shwartz, 2017; Han et al., 2018; Yu et al., 2019; Lyu & Tsang, 2019), our framework requires little computation time for filtering clean instances but does not require any additional parameter to be tuned. Our contributions are summarized as follows:

- We formulate the problem as a system-level framework for *winning ticket hypothesis* that serves as a baseline template to extension for any other robust methods.
- We propose two strategies for identifying winning tickets: **CLK** (Clustering the cross-entropy Loss values into two groups with K-means algorithm) and **SAME** (Selectively Abandon Misaligned data in Eigenspace). **CLK** chooses the bundle of noisy data by using the K-means algorithm based on the cross-entropy loss values, and **SAME** leverages the high-order topological information of data in latent space. Both methods require neither additional learnable parameters nor hyperparameters (Figure 1).
- We show that both **CLK** and **SAME** provide better results for the robust loss function methods (Zhang & Sabuncu, 2018; Wang et al., 2019b; Liu et al., 2020) through the TFT framework. We also improve the performance on the existing sample-selection (Han et al., 2018; Yu et al., 2019) and semi-supervised settings (Li et al., 2019) by applying the CLK and SAME.

1.1. Motivating Examples

Figure 2 shows learning curves of ResNet34 models trained on CIFAR-10 50k examples. The blue line is the case that the labels in the training set are randomly flipped by *symmetric* uniform distribution, and the red line is the case that the noisy samples in the former dataset are segregated. The latter dataset is perfectly clean, but the data points are notably less than the former dataset. In both cases, as the preliminary experiment, we train the models with cross-entropy (CE) loss between the prediction and the labeled one-hot

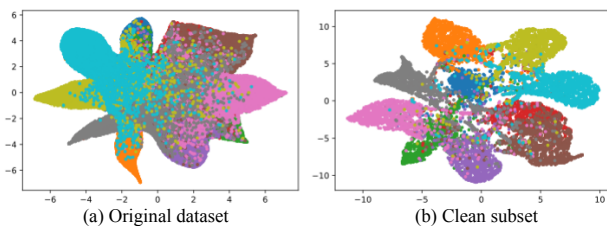


Figure 3. t-SNE visualizations (Van der Maaten & Hinton, 2008) of final features from ResNet34 model trained with cross-entropy (CE) on CIFAR-10 dataset with symmetric noise 80%. (Left) t-SNE visualization of a ResNet34 model on the whole dataset, and (right) t-SNE visualization of a ResNet34 model on the clean samples in the whole dataset.

vector and robust loss function methods (Zhang & Sabuncu, 2018; Wang et al., 2019b; Liu et al., 2020) specifically designed to be robust in the presence of noisy labels with the same training recipe. The details of robust loss function methods are given in section 4. We observe that training a model with the latter dataset has better performance in this setup than with the former dataset despite fewer data points.

Furthermore, we present embeddings of pre-logits (i.e., penultimate layer representation vectors) from CIFAR-10 train samples constructed by t-SNE (Van der Maaten & Hinton, 2008) in Figure 3. It compares the representation of the ResNet34 model trained with CE loss between the original dataset and the clean subset in original. Clusters related to the extracted dataset are separated boundaries while the representation of network with original dataset have poor class separation and clusters have mixed class boundaries. Interestingly, this tendency is consistently observed in the GCE (Zhang & Sabuncu, 2018), SCE (Wang et al., 2019b), and ELR (Liu et al., 2020) loss functions even they are focused on the robust training in noisy conditions. Furthermore, training a model with only clean data accelerates the training in the early stage.

This result motivates us to truncate the noisy samples in training rather than to correct such samples. Therefore, we

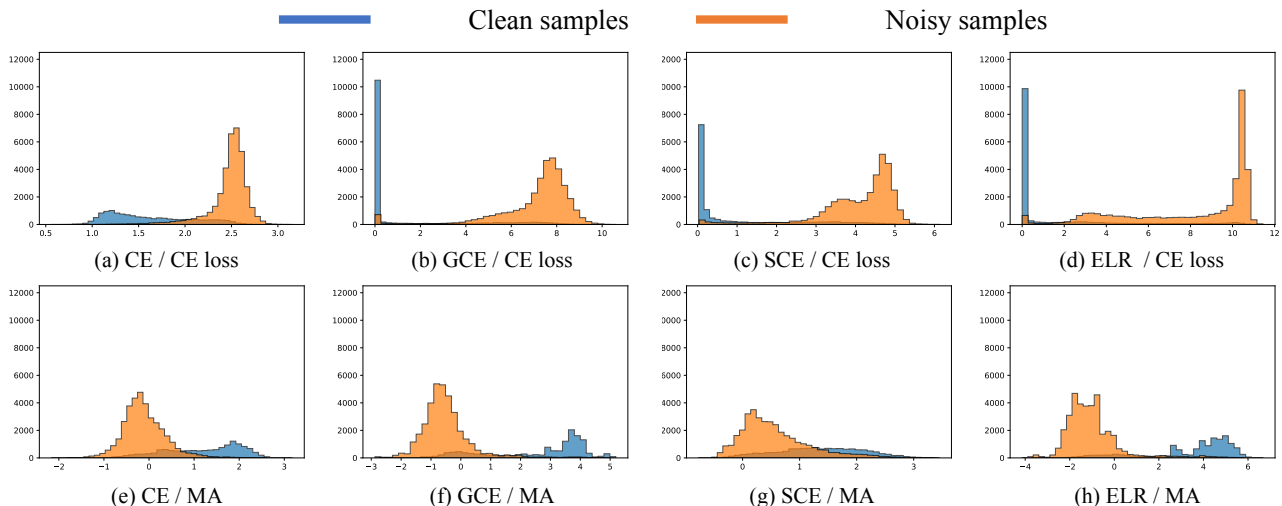


Figure 4. Histograms for the cross-entropy (CE) loss values and misalignment (MA) values, i.e., $|\mathbf{u}_1^\top z| - |\mathbf{u}_2^\top z|$, for the ResNet34 model trained with the robust loss function methods such as CE, GCE, SCE, and ELR on CIFAR-10 with symmetric noise 80%. Blue color indicates the clean samples and orange color is the samples with corrupted label.

focus on purifying the dataset (Wu et al., 2020). To this aim, *sample-selection* methods have attempted to filter the clean data with a specific criterion dynamically during the training process (Wu et al., 2020; Han et al., 2018; Lyu & Tsang, 2019). To the best of our knowledge, this paper is the first work that uses the posterior information from an independent training process to deal with noisy samples.

2. Problem Formulation and Strategies

In this paper, we are interested in clean and noisy prediction. We would like to predict whether data is clean or not by the posterior information of a trained network. By eliminating noisy data, models could improve the performance from the winning ticket hypothesis. Below we present the generic framework of TFT for identifying winning tickets (algorithm 1).

2.1. Problem Formulation

An important thing for NOISYDETECTOR is that noisy data should be excluded while preserving clean data as many as possible in \mathcal{D}_c . We should carefully filter noisy data, since eliminating clean instances, even with removing a large number of noisy data, might hinder training since neural networks get more accurate when the number of data increases.

To assess the quality of noisy detectors, we refer to the *precision* and *recall* for statistical evaluations widely used in anomaly detection and out-of-distribution detection (Hendrycks & Gimpel, 2016; Liang et al., 2017; Lee et al., 2018). The statistical values are functions of the selected clean samples (positive class) and noisy samples (negative

Algorithm 1 Generic framework of TFT

INPUT : \mathcal{D} : data, g : a proxy model parameterized with θ ,
 f : a target model parameterized with w
 OUTPUT : f
 1: Initialize θ^0, w^0 randomly
 /* Phase1: train a proxy model g */
 2: **for** $t \leftarrow 0, \dots, T - 1$ **do**
 3: Sample a mini-batch \mathcal{B} in \mathcal{D}
 4: Update θ^t through a certain robust loss $\mathcal{L}(\mathcal{B}; \theta^{t-1})$
 5: **end for**
 /* Phase2: get clean subset \mathcal{D}_c from \mathcal{D} */
 6: $\mathcal{D}_c \leftarrow \text{NOISYDETECTOR}(\mathcal{D}, g)$
 /* Phase3: train a target model f on \mathcal{D}_c */
 7: **for** $t \leftarrow 0, \dots, T - 1$ **do**
 8: Sample a mini-batch \mathcal{B}_c in \mathcal{D}_c
 9: Update w^t through a certain robust loss $\mathcal{L}(\mathcal{B}_c; w^{t-1})$
 10: **end for**

class). The *precision* indicates the fraction of clean samples among all samples that are predicted as clean, and the *recall* indicates the portion of clean samples that are identified correctly.

2.2. Strategy 1: CE Loss

The noisy instances can be detected by their CE loss values whether or not the CE loss value is larger than a specific threshold (Han et al., 2018; Yu et al., 2019; Wang et al., 2019a), i.e., instances having small losses are classified as clean, and others are classified as noisy. Recently, in (Li et al., 2019), the authors distinguished clean and noisy samples by fitting the Gaussian Mixture Model (GMM) to the CE loss values and predicting their corresponding posterior

Winning Ticket in Noisy Image Classification

Method	Symmetric noise 80%								Asymmetric noise 40%							
	CE		GCE		SCE		ELR		CE		GCE		SCE		ELR	
	CLK	SAME	CLK	SAME	CLK	SAME	CLK	SAME	CLK	SAME	CLK	SAME	CLK	SAME	CLK	SAME
Precision	88.17	33.62	87.40	76.64	84.10	30.39	58.84	67.84	98.01	81.63	93.80	90.27	95.18	90.49	92.84	90.59
Recall	75.29	99.75	84.21	90.66	81.02	96.65	90.04	87.79	92.21	99.95	93.42	98.43	92.39	98.45	89.31	97.62

Table 1. Precision and recall of CLK and SAME for the ResNet34 model trained with the robust loss function methods such as CE, GCE, SCE, and ELR on CIFAR-10 with symmetric noise 80% and asymmetric noise 40%.

probability of the Gaussian component with a smaller loss. However, it is difficult to set the threshold for the posterior probability since the loss distribution is sensitive to the environment, such as the dataset, network, and loss functions (Shu et al., 2020).

We propose a simple yet effective NOISYDETECTOR, called **CLK** (Clustering the CE Loss values into two groups with K -means algorithm), that does not require any threshold. We fit the samples using the k -means algorithm that assigns the instance to the nearest cluster by loss values. We treat the cluster with small mean as a clean subset (first row of Figure 4).

2.3. Strategy 2: Misalignment of Pre-Logits

Recent studies on the distribution of latent representations in deep neural networks provide intuition regarding how correctly the noisy samples can be filtered with the hidden space’s geometrical information. For instance, in (Lee et al., 2018; 2019), the authors proposed frameworks that utilize the topological information of penultimate layer representation (pre-logit) based on the Mahalanobis distance, and, in (Wu et al., 2020), the authors filtered the noisy data based on the Euclidean distance between pre-logits.

Inspired by those works, we propose a novel NOISYDETECTOR that considers the misalignment between pre-logit and the eigenvectors of the pre-logit covariance matrices defined for every class, called **SAME** (Selectively Abandon Misaligned data in Eigenspace). More precisely, **SAME** first creates a covariance matrix of the pre-logit in a noisy-labeled dataset for each class and conducts the eigenvalue decomposition for those covariance matrices. Then, **SAME** finds noisy samples using inner product values between the pre-logits and all the eigenvectors of those corresponding label’s covariance matrix. Suppose the model is well-trained to capture the characteristic of latent space. In that case, clean data will be aligned on the first eigenvector corresponding to the largest eigenvalue while the noisy one is not. Here, we formally define ‘misaligned’ data in Definition 1.

Definition 1. Let x be the data labeled as class k in dataset \mathcal{D} and z be its corresponding pre-logit, and Σ_k be the covariance matrix of all pre-logits labeled as class k in dataset \mathcal{D} i.e., $\Sigma_k = \sum_{z \in \{\text{class}=k\}} z z^\top$. If the data x in

dataset \mathcal{D} is ‘misaligned’ data, then

$$|\mathbf{u}_1^\top z| < \max_{i \neq 1} |\mathbf{u}_i^\top z| \quad (1)$$

Where \mathbf{u}_i is the first and second column of \mathbf{U}_k from the eigenvalue decomposition of Σ_k , i.e., $\Sigma_k = \mathbf{U}_k \Lambda_k \mathbf{U}_k^\top$ when the eigenvalues are in descending order.

In **SAME** (algorithm 2), the data is regarded as noisy if the pre-logit is misaligned (second row of Figure 4). To justify the relationship between the misaligned data and the noisy data, we also establish theoretical evidence that the **SAME** algorithm can approximate the real eigenvectors with small error under some assumptions for its analytic tractability (Theorem 1). Theorem 1 offers intuition regarding the upper bound of perturbation on the first eigenvector as the number of noisy instances (i.e., $m_{k,t}$) becomes smaller and as the angle between aligned vectors (i.e., $\theta_{k,t}$) becomes closer to be orthogonal. The details of the proofs can be found in the Appendix C.

Algorithm 2 SAME Algorithm for NOISYDETECTOR

INPUT : \mathcal{D} : data, g : a proxy model, K : the number of classes

OUTPUT : \mathcal{D}_c : filtered samples

- 1: Initialize the covariance matrix Σ_k to zero matrix $\mathbf{0}$ for all class $k \in 0, \dots, K - 1$
- 2: **for** $(\mathbf{x}_i, \mathbf{y}_i) \in \mathcal{D}$ **do**
- 3: $\mathbf{z}_i \leftarrow$ pre-logit of $g(\mathbf{x}_i)$
- 4: Update the covariance matrix of each class: $\Sigma_{\mathbf{y}_i} \leftarrow \Sigma_{\mathbf{y}_i} + \mathbf{z}_i \mathbf{z}_i^\top$
- 5: **end for**
- 6: **for** $k \leftarrow 0, \dots, K - 1$ **do**
- 7: $\mathbf{U}_k, \Lambda_k \leftarrow$ EIGENVALUE DECOMPOSITION OF Σ_k
- 8: **end for**
- 9: Initialize the set $\mathcal{D}_c \leftarrow \emptyset$
- 10: **for** $(\mathbf{x}_i, \mathbf{y}_i) \in \mathcal{D}$ **do**
- 11: $\mathbf{z}_i \leftarrow$ pre-logit of $g(\mathbf{x}_i)$
- 12: **if** $|\mathbf{u}_{k,1}^\top \mathbf{z}_i| > \max_{i \neq 1} |\mathbf{u}_{k,i}^\top \mathbf{z}_i|$ **then**
- 13: $\mathcal{D}_c \leftarrow \mathcal{D}_c \cup (\mathbf{x}_i, \mathbf{y}_i)$
- 14: **end if**
- 15: **end for**

Theorem 1. Assume that the pre-logits of all instances with true class k are aligned on the unit vector \mathbf{w}_k with the white noise; the expectation of pre-logits with true class k ,

Winning Ticket in Noisy Image Classification

Datasets (Architecture)	Methods	Symmetric label noise				Asymmetric label noise			
		20%	40%	60%	80%	10%	20%	30%	40%
CIFAR-10 (ResNet34)	CE	91.38	88.43	83.89	70.84	93.54	92.55	91.85	90.05
	CE + CLK	93.20	91.46	87.58	75.30	93.88	93.07	92.46	90.20
	CE + SAME	92.47	90.27	85.04	73.02	93.36	92.90	91.51	90.35
	GCE (Zhang & Sabuncu, 2018)	91.34	89.13	85.40	74.75	91.61	91.18	89.22	86.21
	GCE + CLK	91.46	89.06	86.16	79.17	91.95	91.13	90.02	86.62
	GCE + SAME	91.25	89.33	86.44	78.68	91.78	91.52	90.31	88.33
	SCE (Wang et al., 2019b)	89.57	86.93	83.38	71.30	91.18	90.14	88.81	85.94
	SCE + CLK	90.16	88.43	84.47	75.83	90.97	90.82	89.52	86.66
	SCE + SAME	90.35	88.76	84.57	75.01	91.07	91.23	89.57	88.56
	ELR (Liu et al., 2020)	91.99	89.71	86.89	74.97	93.99	92.53	91.69	90.89
	ELR + CLK	92.44	90.80	88.30	79.20	93.94	93.03	92.10	90.48
	ELR + SAME	92.46	91.01	88.04	78.11	93.86	93.47	92.50	91.14
CIFAR-100 (ResNet34)	CE	64.03	53.24	44.96	23.37	73.66	71.45	66.12	55.72
	CE + CLK	72.23	67.57	58.76	29.34	74.52	71.65	63.02	50.44
	CE + SAME	64.32	53.72	45.24	24.31	74.61	71.86	66.41	56.36
	GCE (Zhang & Sabuncu, 2018)	68.92	64.03	54.27	30.78	70.83	68.17	63.01	48.75
	GCE + CLK	69.02	64.88	54.90	33.25	71.51	69.12	65.16	52.66
	GCE + SAME	69.28	64.43	54.33	31.00	71.12	69.00	63.62	50.07
	SCE (Wang et al., 2019b)	63.26	53.16	46.33	23.22	71.90	65.65	57.95	49.88
	SCE + CLK	64.55	66.54	56.68	26.80	74.29	69.44	61.79	47.42
	SCE + SAME	63.66	54.10	46.43	23.96	73.95	68.24	60.38	52.62
	ELR (Liu et al., 2020)	74.25	68.05	54.59	26.32	74.92	74.79	74.63	73.73
	ELR + CLK	73.25	69.97	61.54	36.88	73.89	72.63	71.34	70.47
	ELR + SAME	74.85	69.15	62.16	26.90	75.49	74.63	74.66	73.82

Table 2. Comparison with state-of-the-art methods on CIFAR-10 and CIFAR-100 with symmetric and asymmetric label noise with the addition of CLK and SAME. For using CLK and SAME, we filter the dataset via the network trained with corresponding robust loss method and noisy rate dataset. The best results sharing the same noisy rate and objective function are highlighted in bold.

i.e., $\mathbb{E}_{\mathbf{z} \in \{\text{true class} = k\}}(\mathbf{z})$, is $c_k \mathbf{w}_k$ where c_k is a constant. Additionally, we assume that all c_k have same value as c . Let $n_k, m_{k,t}$ be the number of correctly labeled instances with class k and noisy instances labeled k whose true class is t , respectively. Then, with the \mathbf{v}_k that is the first column of \mathbf{U}_k from the eigenvalue decomposition of Σ_k , the **perturbation** (*i.e.* 2-norm for difference of projection matrices; left hand side of Eq. (2)) holds:

$$\|\mathbf{w}_k \mathbf{w}_k^\top - \mathbf{v}_k \mathbf{v}_k^\top\|_2 \leq \frac{\frac{1}{m_k + n_k} \sum_{t=1}^K m_{k,t} \cdot \sin \theta_{k,t}}{1 - \frac{1}{m_k + n_k} \sum_{t=1}^K m_{k,t} \cdot \sin \theta_{k,t}}, \quad (2)$$

where $m_k = \sum_{t=1}^K m_{k,t}$ and $\theta_{k,t} = \angle(\mathbf{w}_k, \mathbf{w}_t)$.

2.4. Results

We further evaluate the validity of CLK and SAME with precision and recall (Table 1). As shown in Table 1, CLK method has consistently higher precision values than SAME on robust loss function methods, while recall values of CLK are consistently lower than SAME in both simulated noisy datasets. In particular, this tendency is more apparent in asymmetric noise settings. These results imply that CLK and SAME have different advantages for noisy detection.

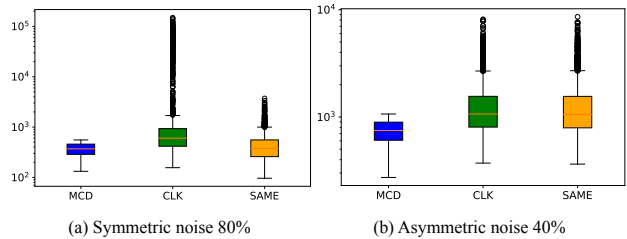


Figure 5. The box plot for the magnitudes of the Mahalanobis distance on the filtered datasets via MCD (Lee et al., 2019), CLK, and SAME. We measure the Mahalanobis distance magnitudes on ‘truck’ class data through the models trained with ELR in Table 2.

CLK attempts to keep the portion of clean data in the truncated dataset more pure than SAME. On the other side, most of the data discarded through the SAME method is noisy data, which shows that it is more pure than CLK. In summary, noisy samples sufficiently differ in either loss landscape or topological features from clean data, and thus CLK and SAME are sufficient to get winning tickets.

Mahalanobis Distance We also verify our CLK and SAME’s superiority compared to the recent robust NOISY-DETECTOR based on the Mahalanobis distance of pre-

Winning Ticket in Noisy Image Classification

Datasets (Architecture)	Symmetric label noise				Asymmetric label noise			
	20%	40%	60%	80%	10%	20%	30%	40%
CIFAR-10 (ResNet34)	CE + CLK 93.20	CE + CLK 91.46	ELR + CLK 88.30	ELR + CLK 79.20	ELR 93.99	ELR + SAME 93.47	ELR + SAME 92.50	ELR + SAME 91.14
CIFAR-100 (ResNet34)	ELR + SAME 74.85	ELR + CLK 69.97	ELR + SAME 62.16	ELR + CLK 36.88	ELR + SAME 75.49	ELR 74.79	ELR + SAME 74.66	ELR + SAME 73.82

Table 3. SOTA methods of Table 2 on CIFAR-10 and CIFAR-100 simulated with different noise setting.

logits (Lee et al., 2019). In (Lee et al., 2019), the authors demonstrated that noisy data might be discriminated from the original dataset based on Mahalanobis distance. They attained performance gain by constructing a generative classifier to get clean samples by estimating the minimum covariance determinant (MCD) of pre-logits in the inference stage with re-training. When evaluating the precision and recall of the MCD method, MCD has significantly worse scores than CLK and SAME reported in Table 1. In 80% symmetric noise and 40% asymmetric noise settings, the precision and recall of MCD applying to pre-logits are 28.44% and 71.28%, and 88.01% and 75.55%, respectively. We visualize the Mahalanobis distance magnitudes on the filtered datasets via MCD, CLK, and SAME (Figure 5). As shown in Figure 5, CLK and SAME methods seem to have compact Mahalanobis distances’ distribution as much as MCD with some outliers.

3. Noisy image classification with Winning Ticket

This section empirically studies how much the winning ticket, obtained by CLK and SAME, can improve existing robust noisy classification algorithms.

Noisy Benchmark Dataset Following the setups of (Zhang & Sabuncu, 2018; Liu et al., 2020), we consider two types of random noisy labels: injecting uniform randomness into a fraction of labels (symmetric) and corrupting a label only to a specific class (asymmetric). For example, we generate noise by mapping TRUCK → AUTOMOBILE, BIRD → AIRPLANE, DEER → HORSE, CAT ↔ DOG to make asymmetric noise for CIFAR-10. For CIFAR-100, we create 20 5-size super-classes and generate asymmetric noise by changing each class to the next class within super-classes circularly.

Hyperparameter Settings We train ResNet34 models with a momentum optimizer for the robust loss function methods such as CE, GCE, SCE, and ELR. Specifically, we set the momentum parameter to 0.9 and the batch size to 128, regardless of the filtering. Regarding the training schedule and hyperparameters, we follow the settings in the original papers (Zhang & Sabuncu, 2018; Liu et al., 2020). For Co-teaching (Han et al., 2018) and DivideMix (Li et al., 2019), we use a PreActResNet18 model and share the same

Methods	Noisy Detector	Sym 80%		Asym 40%	
		Random Init	Fine-tune	Random Init	Fine-tune
CE	CLK	75.30	75.76	90.20	91.30
	SAME	73.02	75.35	90.35	86.57
GCE	CLK	79.17	80.99	86.62	87.44
	SAME	78.68	80.36	88.33	89.21
SCE	CLK	75.83	77.04	86.66	87.47
	SAME	75.01	74.92	88.56	89.02
ELR	CLK	79.20	80.61	90.48	90.65
	SAME	78.11	81.19	91.14	91.48

Table 4. Results on random re-initialization and fine-tuning for the target network on CIFAR-10.

training recipe in the original papers. We provide the more detailed experimental setups in the supplementary material.

3.1. Collaboration with Robust Loss Function Methods

This subsection evaluates our strategies on CIFAR-10 and CIFAR-100 with different levels of symmetric and asymmetric label noise. We compare the collaboration effect of CLK and SAME with various loss functions: CE, SCE (Wang et al., 2019b), GCE (Zhang & Sabuncu, 2018), and ELR (Liu et al., 2020). For the evaluations, there are a lot of possible combinations of the proxy network and the target network in algorithm 1. Here, we focus on the specific case having the same architecture for both networks. We use ResNet34 for the evaluation and re-initialize the target model before training on the filtered dataset.

Table 2 shows the performance of all the models when either CLK or SAME is applied. One intriguing remark is that when using the hyperparameter settings such as weight decay mentioned in (Liu et al., 2020), we can improve the baseline performance than the original papers’ results in (Zhang & Sabuncu, 2018; Wang et al., 2019b; Liu et al., 2020). More interestingly, the models trained with CE seem to be much more robust to label noise than the results reported so far. Our frameworks generally obtain the winning ticket with higher accuracy than existing methods’ performance, suggesting our framework’s robustness with many different robust loss functions. It is hard to assert which one is better between CLK and SAME, which depends on the loss function and noise settings.

Table 3 summarizes the SOTA methods on different noise

Winning Ticket in Noisy Image Classification

Datasets (Architecture)	Methods	Symmetric label noise				Asymmetric label noise			
		20%	40%	60%	80%	10%	20%	30%	40%
CIFAR-10 (PreAct ResNet18)	Co-teaching	89.29	86.18	82.29	71.69	93.00	92.26	91.26	87.69
	Co-teaching + CLK	91.65	89.80	86.27	77.16	92.97	92.17	91.10	89.21
	Co-teaching + SAME	90.62	88.06	83.84	76.03	92.92	92.57	91.44	87.86
	Co-teaching+	89.16	86.06	82.11	63.75	91.64	90.28	88.82	86.40
	Co-teaching+ + CLK	90.68	88.75	85.31	75.96	91.77	91.36	90.71	88.68
	Co-teaching+ + SAME	90.02	88.05	83.80	74.31	92.24	91.06	89.43	86.57
CIFAR-100 (PreAct ResNet18)	Co-teaching	61.37	50.11	37.93	20.08	66.14	59.83	54.41	44.74
	Co-teaching + CLK	67.61	61.56	51.04	30.60	68.89	67.01	68.06	64.62
	Co-teaching + SAME	60.85	52.16	38.09	19.98	70.50	67.84	60.86	48.56
	Co-teaching+	57.80	50.02	36.81	20.22	65.15	59.00	53.84	44.57
	Co-teaching+ + CLK	66.75	60.29	47.06	29.79	67.35	65.41	62.53	58.38
	Co-teaching+ + SAME	59.17	49.41	34.45	26.27	68.66	66.86	59.88	49.38

Table 5. Results of Co-teaching families (Han et al., 2018; Yu et al., 2019) on CIFAR-10 and CIFAR-100 with symmetric and asymmetric label noise with the addition of CLK and SAME. Here, we filter the dataset via the ResNet34 trained with CE (CIFAR-10) / ELR (CIFAR-100) and corresponding noisy rate dataset. The best results sharing the same noisy rate and method are highlighted in bold.

Methods	Noisy Detector	Iteration					
		Sym 80%			Asym 40%		
		1	2	3	1	2	3
CE	CLK	75.30	75.75	75.49	90.20	90.16	90.14
	SAME	73.02	72.36	71.84	90.35	90.53	90.74
GCE	CLK	79.17	30.52	NaN	86.62	NaN	-
	SAME	78.68	79.12	78.25	88.33	NaN	-
SCE	CLK	75.83	75.85	76.24	86.66	86.53	86.45
	SAME	75.01	69.15	69.08	88.56	88.57	88.77
ELR	CLK	79.20	79.34	79.14	90.48	90.75	90.86
	SAME	78.11	78.70	74.08	91.14	91.40	91.56

Table 6. Results of iterative filtering on symmetric noise 80% and asymmetric noise 40% of CIFAR-10.

settings listed in Table 2. Interestingly, CE is also a useful loss function that is robust to noisy samples with our framework. In particular, it is observed that ELR gains more benefit from our frameworks; SAME has more synergy with the ELR than CLK. We think that the temporal ensembling technique in the ELR method could make the alignments of pre-logits more informative.

Initialization Next, we investigate how an initialization for the target network affects the performance when reusing the same architecture for the proxy network for NOISYDETECTOR and the target network. For different noise settings of CIFAR-10, we evaluate two following cases: (1) fine-tuning with the initial training recipe and (2) retraining with re-initialization. In Table 4, we find that fine-tuning with the initial training recipe is better than re-initialization when using the same architecture for the proxy network and the target network.

Iterative Filtering Table 6 shows the behavior with respect to the filtering level when algorithms purify the data iteratively. At the n -th iteration, we filter the dataset used

in the $n - 1$ -th iteration, and at every iteration, we retrain the model. We observe that the iterative filtering facilitates more generalization in some cases, but we cannot find consistency. Even with GCE, the models are not trained well due to their sensitivity of hyperparameters. After a certain level, CLK and SAME iterations hinder the training because CLK and SAME even attempt to segregate the data when neither noisy data remains.

3.2. Collaboration with Co-teaching Families

Our general filtering methods provide benefits to a variety of robust methods. A possible application is a case that there are two networks such that one of them extracts a set of instances with small losses, and the other one is trained with the extracted set. Co-teaching (Han et al., 2018) and Co-teaching+ (Yu et al., 2019)¹ are the case. They solve learning bias in training by utilizing those two networks that generate different learning decision boundaries and have different learning abilities.

We compare the performances of the Co-teaching families with and without CLK or SAME in Table 5. To combine our filtering methods and Co-teaching families, unlike the original methods that update parameters to reduce cross-entropy loss for all instances, we train the model to reduce cross-entropy only for filtered instances. We utilize a ResNet34 model for the training in subsection 3.1 as the proxy network. The implementation details for Co-teaching families are in the Appendix D. Table 5 shows that our frameworks constantly outperform the baseline under most of the noise settings.

¹We used a reference implementation: <https://github.com/bhanML/Co-teaching>

Method	Sym 20%	Sym 90%	Asym 40%
DivideMix	96.1	76.0	93.4
DivideMix + CLK	96.1	73.1	93.2
DivideMix + SAME	96.1	79.7	94.3

Table 7. Collaboration results between DivideMix (Li et al., 2019) and CLK and SAME on different noise settings of CIFAR-10.

3.3. Collaboration with DivideMix

To further assess the generalization capacity of CLK and SAME, we apply our framework to DivideMix (Li et al., 2019)² which is one of the most potent *semi-supervised* approaches in noise settings. DivideMix (Li et al., 2019) models the per-sample loss distribution to divide into a labeled set with clean samples and an unlabeled set with noisy samples, and leverage the noisy samples through semi-supervised learning technique MixMatch (Berthelot et al., 2019). There are two networks that have similar purpose with Co-teaching families and additional efficient strategies for the MixMatch such as label co-refinement and label co-guessing on labeled and unlabeled samples, respectively.

We experiment DivideMix by substituting its segregation process with the CLK and SAME; we select clean samples through CLK and SAME of each network. The implementation details are described in the Appendix D. We report the results in Table 7 and observe consistent performance gains by applying the SAME compared to the baseline. This result demonstrates that SAME is beneficial for DivideMix.

4. Related Works

Robust Training Method Numerous works have been studied for the classification task with noisy labels. (Ghosh et al., 2017) showed that the mean absolute error (MAE) might be robust against noisy labels. (Zhang & Sabuncu, 2018) argued that MAE performed poorly with DNNs and proposed a GCE loss function, which can be seen as a generalization of MAE and CE. (Wang et al., 2019b) introduced the reverse version of the cross-entropy term (RCE) and suggested the SCE loss function as a weighted sum of CE and RCE. (Liu et al., 2020) found that the network learns to predict the clean instances in the early learning phase correctly. From this intuition, they proposed an ELR loss function to prohibit memorizing noisy data. (Han et al., 2018) suggested a Co-teaching framework that extracts subsets of instances with small losses from each network and trained on subsets of instances filtered by another network. (Yu et al., 2019) combined disagreement training procedure, which only selects instances predicted differently by two networks to Co-teaching. Recently, (Wu et al., 2020) proposed a method called TopoFilter that filters the noisy data by utilizing the k-nearest neighborhood algorithm and Eu-

²We reproduced the code through <https://github.com/LiJunnan1992/DivideMix>.

clidean distance between pre-logits. (Mirzasoileman et al., 2020) introduced an algorithm that selects subsets of clean instances that provide an approximately low-rank Jacobian matrix and proved that gradient descent applied to the subsets prevents overfitting to noisy labels. (Pleiss et al., 2020) proposed an area under margin (AUM) statistic that measures the average difference between the logit values of the assigned class and its highest non-assigned class to divide clean and noisy samples. (Xia et al., 2021) presented a framework that divides the model parameters into two part: which parameters tend to fit data with clean labels and noisy labels.

Dataset Resampling Data resampling is a common technique that extracts a new dataset from the distribution of the original dataset to remove the dataset bias in the machine learning community. In class-imbalance tasks, numerous literature conducted over-sampling the minority classes (Chawla et al., 2002; Ando & Huang, 2017) or under-sampling the majority classes (Buda et al., 2018) to balance the number of data per class. (Li & Vasconcelos, 2019) proposed a resampling procedure to reduce the representation bias of the data by learning a weight distribution that favors difficult instances for a given feature representation. (Le Bras et al., 2020) suggested adversarial filtering based approach to remove spurious artifacts in the dataset. Analogously, in anomaly detection and out-of-distribution detection problems (Hendrycks & Gimpel, 2016; Liang et al., 2017; Lee et al., 2018), the malicious data is usually detected by looking at the loss value or negative behavior in feature representation space. While our research is motivated by such previous works, this paper focuses on the noisy image classification task.

5. Conclusion

This paper states the *winning ticket hypothesis* that a model trained on the dataset possessing the bundle of clean samples from the original dataset has better performance than the network trained on the original dataset. Based on the winning ticket hypothesis, we propose a train-filter-train training flow, a novel training strategy that (1) trains a proxy model on the dataset, (2) segregates the noisy instances via the posterior information from the proxy model, and (3) trains the target model on the segregated dataset. We propose two effective strategies to get the winning ticket, referred to as **CLK** and **SAME**, respectively. **CLK** clusters the cross-entropy loss values of all instances into two groups via the k-means algorithm and **SAME** leverages the topological property of the data in the eigenspace of pre-logits. We also present theoretical evidence that the **SAME** can select clean data. We empirically show that combining our strategies with a variety of existing robust methods improves test accuracies. We expect that our framework will provide better optima when a model is trained with various noisy robust methods in simple and effective manners.

References

- Ando, S. and Huang, C. Y. Deep over-sampling framework for classifying imbalanced data. In *Joint European Conference on Machine Learning and Knowledge Discovery in Databases*, pp. 770–785. Springer, 2017.
- Berthelot, D., Carlini, N., Goodfellow, I., Papernot, N., Oliver, A., and Raffel, C. A. Mixmatch: A holistic approach to semi-supervised learning. In *Advances in Neural Information Processing Systems*, pp. 5049–5059, 2019.
- Buda, M., Maki, A., and Mazurowski, M. A. A systematic study of the class imbalance problem in convolutional neural networks. *Neural Networks*, 106:249–259, 2018.
- Chawla, N. V., Bowyer, K. W., Hall, L. O., and Kegelmeyer, W. P. Smote: synthetic minority over-sampling technique. *Journal of artificial intelligence research*, 16:321–357, 2002.
- Ghosh, A., Kumar, H., and Sastry, P. Robust loss functions under label noise for deep neural networks. *arXiv preprint arXiv:1712.09482*, 2017.
- Han, B., Yao, Q., Yu, X., Niu, G., Xu, M., Hu, W., Tsang, I., and Sugiyama, M. Co-teaching: Robust training of deep neural networks with extremely noisy labels. In *Advances in neural information processing systems*, pp. 8527–8537, 2018.
- He, K., Zhang, X., Ren, S., and Sun, J. Deep residual learning for image recognition. In *Proceedings of the IEEE conference on computer vision and pattern recognition*, pp. 770–778, 2016.
- Hendrycks, D. and Gimpel, K. A baseline for detecting misclassified and out-of-distribution examples in neural networks. *arXiv preprint arXiv:1610.02136*, 2016.
- Jiang, L., Zhou, Z., Leung, T., Li, L.-J., and Fei-Fei, L. Mentornet: Learning data-driven curriculum for very deep neural networks on corrupted labels. In *International Conference on Machine Learning*, pp. 2304–2313. PMLR, 2018.
- Krizhevsky, A., Sutskever, I., and Hinton, G. E. Imagenet classification with deep convolutional neural networks. *Advances in neural information processing systems*, 25: 1097–1105, 2012.
- Le Bras, R., Swayamdipta, S., Bhagavatula, C., Zellers, R., Peters, M., Sabharwal, A., and Choi, Y. Adversarial filters of dataset biases. In *International Conference on Machine Learning*, pp. 1078–1088. PMLR, 2020.
- Lee, K., Lee, K., Lee, H., and Shin, J. A simple unified framework for detecting out-of-distribution samples and adversarial attacks. In *Advances in Neural Information Processing Systems*, pp. 7167–7177, 2018.
- Lee, K., Yun, S., Lee, K., Lee, H., Li, B., and Shin, J. Robust inference via generative classifiers for handling noisy labels. *arXiv preprint arXiv:1901.11300*, 2019.
- Li, J., Socher, R., and Hoi, S. C. Dividemix: Learning with noisy labels as semi-supervised learning. In *International Conference on Learning Representations*, 2019.
- Li, Y. and Vasconcelos, N. Repair: Removing representation bias by dataset resampling. In *Proceedings of the IEEE/CVF Conference on Computer Vision and Pattern Recognition*, pp. 9572–9581, 2019.
- Liang, S., Li, Y., and Srikant, R. Enhancing the reliability of out-of-distribution image detection in neural networks. *arXiv preprint arXiv:1706.02690*, 2017.
- Liu, S., Niles-Weed, J., Razavian, N., and Fernandez-Granda, C. Early-learning regularization prevents memorization of noisy labels. *Advances in Neural Information Processing Systems*, 33, 2020.
- Lyu, Y. and Tsang, I. W. Curriculum loss: Robust learning and generalization against label corruption. *arXiv preprint arXiv:1905.10045*, 2019.
- Malach, E. and Shalev-Shwartz, S. Decoupling” when to update” from” how to update”. In *Advances in Neural Information Processing Systems*, pp. 960–970, 2017.
- Mirzasoleiman, B., Cao, K., and Leskovec, J. Coresets for robust training of neural networks against noisy labels. *arXiv preprint arXiv:2011.07451*, 2020.
- Pleiss, G., Zhang, T., Elenberg, E. R., and Weinberger, K. Q. Identifying mislabeled data using the area under the margin ranking. *arXiv preprint arXiv:2001.10528*, 2020.
- Shu, J., Zhao, Q., Chen, K., Xu, Z., and Meng, D. Learning adaptive loss for robust learning with noisy labels. *arXiv preprint arXiv:2002.06482*, 2020.
- Van der Maaten, L. and Hinton, G. Visualizing data using t-sne. *Journal of machine learning research*, 9(11), 2008.
- Wang, X., Wang, S., Wang, J., Shi, H., and Mei, T. Co-mining: Deep face recognition with noisy labels. In *Proceedings of the IEEE international conference on computer vision*, pp. 9358–9367, 2019a.
- Wang, Y., Ma, X., Chen, Z., Luo, Y., Yi, J., and Bailey, J. Symmetric cross entropy for robust learning with noisy labels. In *Proceedings of the IEEE International Conference on Computer Vision*, pp. 322–330, 2019b.

- Wu, P., Zheng, S., Goswami, M., Metaxas, D., and Chen, C. A topological filter for learning with label noise. *arXiv preprint arXiv:2012.04835*, 2020.
- Xia, X., Liu, T., Han, B., Gong, C., Wang, N., Ge, Z., and Chang, Y. Robust early-learning: Hindering the memorization of noisy labels. In *International Conference on Learning Representations*, 2021. URL https://openreview.net/forum?id=Eql5b1_hTE4.
- Yu, X., Liu, T., Gong, M., and Tao, D. Learning with biased complementary labels. In *Proceedings of the European conference on computer vision (ECCV)*, pp. 68–83, 2018.
- Yu, X., Han, B., Yao, J., Niu, G., Tsang, I. W., and Sugiyama, M. How does disagreement help generalization against label corruption? *arXiv preprint arXiv:1901.04215*, 2019.
- Zhang, C., Bengio, S., Hardt, M., Recht, B., and Vinyals, O. Understanding deep learning requires rethinking generalization. *arXiv preprint arXiv:1611.03530*, 2016.
- Zhang, Z. and Sabuncu, M. Generalized cross entropy loss for training deep neural networks with noisy labels. *Advances in neural information processing systems*, 31: 8778–8788, 2018.

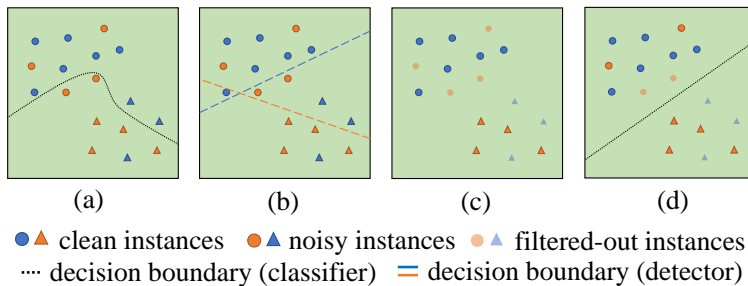


Figure 6. An overview of TFT; (a) train a proxy model with noisy samples making vulnerable decision boundary, (b) utilize a proxy model as a NOISYDETECTOR to classify clean and noisy samples, (c) generate new dataset with the samples identified as clean by the NOISYDETECTOR (opaque shapes), (d) train a target network with the extracted dataset.

A. Overview of TFT

Figure 6 depicts the overview of TFT. In Figure 6, the geometrical shape of each instance represents the different true class and the color indicates the marked label. By using a proxy model for a NOISYDETECTOR, we believe that a target network can learn robust classifiers towards the noisy instances (Figure 6 (d)).

B. Further Related Work

Numerous works have been studied for the classification task with noisy labels. We further consider the studies regarding robust architecture and loss adjustment.

Robust Architecture Architectural changes in a certain network may mitigate the negative effect of noisy instances. Building a new network with noise adaptation layers is a possible way to increase performance. Generally, a noise adaptation layer is located after the softmax layer and it is not utilized in the inference phase. In (Chen & Gupta, 2015), the authors utilized the concept of curriculum learning. More precisely, first, they trained a model with easy data that has a small loss value and form a confusion matrix with those data. Then, they initialized weight parameters of the noise adaptation layer with the confusion matrix. Do this progress on every iteration. (Sukhbaatar et al., 2014) set an initial weight matrix of a noise adaptation layer with an identity matrix. With a certain learning rate and enough training time, the noisy adaptation layer absorbs the noise from base model. (Jindal et al., 2016) applied the dropout regularization in the noise adaptation layer to prevent a target model from being over-determined with noisy labels. EM algorithm was implemented in (Bekker & Goldberger, 2016). E-step estimated true labels and M-step updated parameters with back propagation.

Loss Adjustment Various literature has been studied for direct loss adjustment method to remedy the negative impact of noisy samples. In (Patrini et al., 2017), the authors directly corrected the loss value by multiplying the inverse of the estimated transition matrix T . In (Wang et al., 2017), the authors modified importance reweighting procedure of (Patrini et al., 2017) to compute the ratio of two joint data distributions for assigning less importance to noisy samples and higher importance to clean samples.

C. Theoretical Guarantee of the Algorithm

This section provides the detailed proof of Theorem 1.

C.1. Preliminaries

Spectral Norm In this section, we frequently use the spectral norm. For any matrix $A \in \mathbb{R}^{m \times n}$, the spectral norm are defined as follows:

$$\|A\|_2 = \sup_{x \in \mathbb{R}^n: \|x\|=1} \|Ax\|,$$

where a_{ij} is the (i, j) element of A .

Singular Value Decomposition (SVD) Let $A \in \mathbb{R}^{m \times n}$. There exist orthogonal matrices that satisfy the following:

$$\begin{aligned}
 U &= [u_1, u_2, \dots, u_m] \in \mathbb{R}^{m \times m} \quad \text{and} \quad V = [v_1, v_2, \dots, v_n] \in \mathbb{R}^{n \times n} \\
 \text{such that} \quad U^\top AV &= \text{diag}[\sigma_1, \sigma_2, \dots, \sigma_{\min\{m,n\}}]
 \end{aligned} \tag{3}$$

where $\sigma_1 \geq \sigma_2 \geq \dots \geq \sigma_{\min\{m,n\}}$ which are called singular values and $\text{diag}[\cdot]$ is a diagonal matrix whose diagonal consists of the vector in the bracket $[\cdot]$. (Note that $UU^\top = U^\top U = I$ when U is an orthogonal matrix).

C.2. Lemmas for Theorem 1

We dealt with the lemmas used for the proof of [Theorem 1](#).

Lemma 1. *Let V and W be orthogonal matrices and $V = [V_1, V_2]$ and $W = [W_1, W_2]$ with $V_1, W_1 \in \mathbb{R}^{n \times k}$. Then, we have*

$$\|V_1 V_1^\top - W_1 W_1^\top\|_2 = \|V_1^\top W_2\|_2 = \|V_2^\top W_1\|_2.$$

Proof. From the orthogonal invariance property,

$$\begin{aligned}
 \|V_1 V_1^\top - W_1 W_1^\top\|_2 &= \|V^\top (V_1 V_1^\top - W_1 W_1^\top) W\|_2 \\
 &= \left\| \begin{bmatrix} 0 & V_1^\top W_2 \\ -V_2^\top W_1 & 0 \end{bmatrix} \right\|_2 \\
 &= \max\{\|V_1^\top W_2\|_2, \|V_2^\top W_1\|_2\},
 \end{aligned}$$

where the last line can be obtained from $\|A\|_2^2 = \max_{x \in \mathbb{R}^n: \|x\|_2=1} \|Ax\|_2^2$.

Thus, to conclude this proof, it suffices to show that $\|V_1^\top W_2\|_2 = \|V_2^\top W_1\|_2$.

Since $W_1 W_1^\top + W_2 W_2^\top = I$,

$$\begin{aligned}
 \|V_1^\top W_2\|_2^2 &= \max_{x \in \mathbb{R}^k: \|x\|_2=1} x^\top V_1^\top W_2 W_2^\top V_1 x \\
 &= \max_{x \in \mathbb{R}^k: \|x\|_2=1} x^\top V_1^\top (I - W_1 W_1^\top) V_1 x \\
 &= \max_{x \in \mathbb{R}^k: \|x\|_2=1} 1 - x^\top V_1^\top W_1 W_1^\top V_1 x \\
 &= 1 - \max_{x \in \mathbb{R}^k: \|x\|_2=1} x^\top V_1^\top W_1 W_1^\top V_1 x \\
 &= 1 - \lambda_k(V_1^\top W_1 W_1^\top V_1) \\
 &= 1 - \sigma_k(V_1^\top W_1)^2,
 \end{aligned}$$

where $\sigma_k(V_1^\top W_1)$ is the k -th singular value of $V_1^\top W_1$. Analogously, we can show that

$$\|W_1^\top V_2\|_2^2 = 1 - \sigma_k(V_1^\top W_1)^2.$$

Thus, we have

$$\|V_1 V_1^\top - W_1 W_1^\top\|_2 = \|V_1^\top W_2\|_2 = \|V_2^\top W_1\|_2 = \sqrt{1 - \sigma_k(V_1^\top W_1)^2}.$$

□

Lemma 2. (Weyl's Theorem) For any real matrices $A, B \in \mathbb{R}^{m \times n}$,

$$\sigma_i(A + B) \leq \sigma_i(A) + \sigma_1(B).$$

Proof. From the definition of the SVD, for any given matrix $X \in \mathbb{R}^{m \times n}$.

$$\begin{aligned} \sigma_i(X) &= \sup_{V: \dim(V)=i} \inf_{v \in V: \|v\|_2=1} \|v^T(A+B)\|_2 \\ &\leq \sup_{V: \dim(V)=i} \inf_{v \in V: \|v\|_2=1} \|v^T A\|_2 + \|v^T B\|_2 \\ &\leq \sup_{V: \dim(V)=i} \inf_{v \in V: \|v\|_2=1} \|v^T A\|_2 + \|B\|_2 \\ &\leq \sigma_i(A) + \sigma_1(B). \end{aligned}$$

□

Lemma 3. (David-Kahan sin Theorem) For given symmetric matrices $A, B \in \mathbb{R}^{n \times n}$, let $A = U\Lambda U^T$ and $A+B = \bar{U}\bar{\Lambda}\bar{U}^T$ be eigenvalue decomposition of A and $A+B$. Then,

$$\|U_{1:k}(U_{1:k})^T - \bar{U}_{1:k}(\bar{U}_{1:k})^T\|_2 \leq \frac{|B|_2}{\lambda_k(A) - \lambda_{k+1}(A) - |B|_2},$$

where $U_{1:k}$ and $\bar{U}_{1:k}$ denote the first k columns of U and \bar{U} , respectively.

Proof. Assume that A and $A+B$ have non-negative eigenvalues. If not, there exists a large enough constant c to make $\tilde{A} + cI$ so that \tilde{A} and $\tilde{A} + B$ become positive semi-definite matrices. Note that A (resp. $A+B$) and \tilde{A} (resp. $\tilde{A} + B$) share the same eigenvectors and eigenvalue gaps $\lambda_i(A) - \lambda_{i+1}(A)$.

From the Lemma 2, we have

$$\lambda_i(A) - |B|_2 \leq \lambda_i(A+B) \leq \lambda_i(A) + |B|_2. \quad (4)$$

Thus,

$$(\lambda_{k+1}(A) + |B|_2) |(\bar{U}_{k+1:n})^T U_{k+1:n}|_2 \not\leq |(\bar{U}_{k+1:n})^T (A+B) U_{1:k}|_2 \quad (5)$$

$$\not\leq |(\bar{U}_{k+1:n})^T A U_{1:k}|_2 - |B|_2 \quad (6)$$

$$\geq \lambda_k(A) |(\bar{U}_{k+1:n})^T U_{1:k}|_2 - |B|_2 \quad (7)$$

From (5), we have

$$\|U_{1:k}(U_{1:k})^T - \bar{U}_{1:k}(\bar{U}_{1:k})^T\|_2 \leq \frac{|B|_2}{\lambda_k(A) - \lambda_{k+1}(A) - |B|_2}.$$

Proof of (3) : Since the columns of $\bar{U}_{k+1:n}$ are singular vectors of $A+B$,

$$(\bar{U}_{k+1:n})^T (A+B) U_{1:k} = \bar{\Lambda}_{k+1:n} (\bar{U}_{k+1:n})^T U_{1:k}.$$

Therefore,

$$\|(\bar{U}_{k+1:n})^T(A+B)U_{1:k}\|_2 \leq \|\bar{\Lambda}_{k+1:n}\|_2 \|(\bar{U}_{k+1:n})^T U_{1:k}\|_2 = \lambda_{k+1}(A+B) \|(\bar{U}_{k+1:n})^T U_{1:k}\|_2$$

From (2), we have $\lambda_{k+1}(A+B) \leq \lambda_{k+1}(A) + \|B\|_2$

Proof of (4) : From the triangle inequality,

$$\begin{aligned} \|(\bar{U}_{k+1:n})^T A U_{1:k}\|_2 &= \|(\bar{U}_{k+1:n})^T (A+B) U_{1:k} + (-\bar{U}_{k+1:n})^T B U_{1:k}\|_2 \\ &\leq \|(\bar{U}_{k+1:n})^T (A+B) U_{1:k}\|_2 + \|(-\bar{U}_{k+1:n})^T B U_{1:k}\|_2. \end{aligned}$$

We have

$$\|(-\bar{U}_{k+1:n})^T B U_{1:k}\|_2 \leq \|(-\bar{U}_{k+1:n})^T\|_2 \|B\|_2 \|U_{1:k}\|_2 = \|B\|_2.$$

Proof of (5) : Since the columns of $U_{1:k}$ are singular vectors of A,

$$(\bar{U}_{k+1:n})^T A U_{1:k} = (\bar{U}_{k+1:n})^T U_{1:k} \Lambda_{1:k}$$

Therefore,

$$\|(\bar{U}_{k+1:n})^T A U_{1:k}\|_2 = \|(\bar{U}_{k+1:n})^T U_{1:k} \Lambda_{1:k}\|_2 \geq \|(\bar{U}_{k+1:n})^T U_{1:k}\|_2 \lambda_k(A).$$

□

C.3. Proof of Theorem 1 and Propositions from Theorem 1

We first prove the Theorem 1 and apply the Theorem 1 on both symmetric and asymmetric noise settings.

Proof. Without loss of generality, it is sufficient to consider only for instances labeled as 0. Then, let A_0 and $A_0 + B_0$ be the projection matrices,

$$\begin{aligned} A_0 &= c^2 \mathbf{w}_0 \mathbf{w}_0^T \\ A_0 + B_0 &= c^2 \left[\frac{n_0}{n_0 + m_0} \mathbf{w}_0 \mathbf{w}_0^T + \frac{m_{0,1}}{m_0} \cdot \frac{m_0}{n_0 + m_0} \mathbf{w}_1 \mathbf{w}_1^T + \dots + \frac{m_{0,K}}{m_0} \cdot \frac{m_0}{n_0 + m_0} \mathbf{w}_K \mathbf{w}_K^T \right] \end{aligned}$$

Then,

$$B_0 = \frac{m_0 c^2}{n_0 + m_0} \left[\frac{m_{0,1}}{m_0} \mathbf{w}_1 \mathbf{w}_1^T + \dots + \frac{m_{0,K}}{m_0} \mathbf{w}_K \mathbf{w}_K^T \right] - \frac{m_0 c^2}{n_0 + m_0} \mathbf{w}_0 \mathbf{w}_0^T$$

Let the term $B_{0,i}$ be as follows:

$$B_{0,i} = \frac{m_{i,0}}{m_0} \cdot \frac{m_0 c^2}{n_0 + m_0} (\mathbf{w}_i \mathbf{w}_i^T - \mathbf{w}_0 \mathbf{w}_0^T)$$

From the Lemma 1, we have

$$\|B_{0,i}\|_2 = \frac{m_{0,i}}{m_0} \cdot \frac{m_0 c^2}{m_0 + n_0} \|\mathbf{w}_i \mathbf{w}_i^T - \mathbf{w}_0 \mathbf{w}_0^T\|_2 = \frac{m_{0,i}}{m_0} \frac{m_0 c^2}{m_0 + n_0} \langle \mathbf{w}_i, \mathbf{w}_0^\perp \rangle = \frac{m_{0,i}}{m_0} \frac{m_0 c^2}{m_0 + n_0} \cdot \sin \theta_{0,i}$$

where $\theta_{0,i}$ is the acute angle between \mathbf{w}_0 and \mathbf{w}_i . From triangular inequality,

$$\|B_0\|_2 = \left\| \sum_{i=1}^K B_{0,i} \right\| \leq \sum_{i=1}^K \|B_{0,i}\| = \frac{m_0 c_0^2}{m_0 + n_0} \sum_{i=1}^K \frac{m_{0,i}}{m_0} \cdot \sin \theta_{0,i}$$

From Lemma 3,

$$\begin{aligned} \|U_{1:k} U_{1:k}^T - \bar{U}_{1:k} (\bar{U}_{1:k})^T\|_2 &\leq \frac{\|B_0\|_2}{\lambda_k(A_0) - \lambda_{k+1}(A_0) - \|B_0\|_2} \\ &\leq \frac{\sum_{i=1}^K \|B_{0,i}\|_2}{\lambda_k(A_0) - \lambda_{k+1}(A_0) - \sum_{i=1}^K \|B_{0,i}\|_2} \\ &= \frac{\frac{m_0 c^2}{m_0 + n_0} \sum_{i=1}^K \frac{m_{0,i}}{m_0} \cdot \sin \theta_{0,i}}{c^2 - \frac{m_0 c^2}{m_0 + n_0} \sum_{i=1}^K \frac{m_{0,i}}{m_0} \cdot \sin \theta_{0,i}} \\ &= \frac{\frac{m_0}{m_0 + n_0} \sum_{i=1}^K \frac{m_{0,i}}{m_0} \cdot \sin \theta_{0,i}}{1 - \frac{m_0}{m_0 + n_0} \sum_{i=1}^K \frac{m_{0,i}}{m_0} \cdot \sin \theta_{0,i}} \end{aligned}$$

□

Based on the Theorem 1, we can estimate the upper bound of the perturbations in symmetric and asymmetric settings (Proposition 1 and Proposition 2).

Proposition 1. (Asymmetric Noise Setting) Let i be the corrupted class from the j class instance. Then, we have the upper bound of perturbation as following:

$$\frac{\frac{m_{i,j}}{m_{i,j} + n_i} \cdot \sin \theta_{i,j}}{1 - \frac{m_{i,j}}{m_{i,j} + n_i} \cdot \sin \theta_{i,j}}$$

Proof. Without loss of generality, it is sufficient to consider only for instances labeled as 0 and assume that class 0 is corrupted only with a class 1 data.

$$\begin{aligned} A &= c \mathbf{w}_0 \mathbf{w}_0^T \\ B &= c^2 \left[\frac{m_{0,1}}{m_{0,1} + n_0} (\mathbf{w}_1 \mathbf{w}_1^T - \mathbf{w}_0 \mathbf{w}_0^T) \right] \end{aligned}$$

From the Lemma 1, we have

$$\begin{aligned} \|B\|_2 &= \frac{m_{0,1} c^2}{m + n} \|\mathbf{w}_1 \mathbf{w}_1^T - \mathbf{w}_0 \mathbf{w}_0^T\|_2 \\ &= \frac{m_{0,1} c^2}{m_{0,1} + n_0} \|\mathbf{w}_1 \mathbf{w}_0^\perp\|_2 = \frac{m_{0,1} c^2}{m_{0,1} + n_0} \langle \mathbf{w}_1, \mathbf{w}_0^\perp \rangle = \frac{m_{0,1} c^2}{m_{0,1} + n_0} \cdot \sin \theta_{0,1}. \end{aligned}$$

From the Lemma 3, we have

$$\begin{aligned} \|U_{1:k} U_{1:k}^T - \bar{U}_{1:k} (\bar{U}_{1:k})^T\|_2 &\leq \frac{\|B\|_2}{\lambda_k(A) - \lambda_{k+1}(A) - \|B\|_2} \\ &= \frac{\|B\|_2}{c^2 - \|B\|_2} = \frac{\frac{m_{0,1}}{m_{0,1} + n_0} \cdot \sin \theta_{0,1}}{1 - \frac{m_{0,1}}{m_{0,1} + n_0} \cdot \sin \theta_{0,1}} \end{aligned}$$

□

Proposition 2. (Symmetric Noise Setting) For class k , we have the upper bound of perturbation as following:

$$\frac{\frac{1}{K} \frac{m_k}{m_k+n_k} \sum_{i=1}^K \sin \theta_{k,i}}{1 - \frac{1}{K} \frac{m_k}{m_k+n_k} \sum_{i=1}^K \sin \theta_{k,i}}$$

Proof. Without loss of generality, it is sufficient to consider only for instances labeled as 0. We have

$$\begin{aligned} A_0 &= c^2 \mathbf{w}_0 \mathbf{w}_0^T \\ A_0 + B_0 &= c^2 \left[\frac{n_0}{n_0 + m_0} \mathbf{w}_0 \mathbf{w}_0^T + \frac{1}{K} \cdot \frac{m_0}{n_0 + m_0} \mathbf{w}_1 \mathbf{w}_1^T + \cdots + \frac{1}{K} \cdot \frac{m_0}{n_0 + m_0} \mathbf{w}_K \mathbf{w}_K^T \right] \end{aligned}$$

since $m_{0,i} = \frac{1}{K} m_0$ for $\forall i$. Then,

$$B = c^2 \left[\frac{1}{K} \cdot \frac{m_0}{n_0 + m_0} (\mathbf{w}_1 \mathbf{w}_1^T + \cdots + \mathbf{w}_K \mathbf{w}_K^T) - \frac{m_0}{n_0 + m_0} \mathbf{w}_0 \mathbf{w}_0^T \right]$$

We define the term $B_{0,i}$

$$B_{0,i} = \frac{1}{K} \cdot \frac{m_0 c^2}{n_0 + m_0} (\mathbf{w}_i \mathbf{w}_i^T - \mathbf{w}_0 \mathbf{w}_0^T)$$

From *Lemma 1*, we have

$$\|B_{0,i}\|_2 = \frac{1}{K} \cdot \frac{m_0 c^2}{m_0 + n_0} \|\mathbf{w}_i \mathbf{w}_i^T - \mathbf{w}_0 \mathbf{w}_0^T\|_2 = \frac{1}{K} \frac{m_0 c^2}{m_0 + n_0} \cdot \sin \theta_{0,i}$$

From triangular inequality,

$$\|B_0\|_2 = \left\| \sum_{i=1}^K B_{0,i} \right\| \leq \sum_{i=1}^K \|B_{0,i}\| = \frac{1}{K} \frac{m_0 c^2}{m_0 + n_0} \sum_{i=1}^K \sin \theta_{0,i}$$

From *Lemma 3*,

$$\begin{aligned} \|U_{1:k} U_{1:k}^T - \bar{U}_{1:k} (\bar{U}_{1:k})^T\|_2 &\leq \frac{|B_0|_2}{\lambda_k(A_0) - \lambda_{k+1}(A_0) - |B_0|_2} \\ &\leq \frac{\sum_{i=1}^K \|B_{0,i}\|_2}{\lambda_k(A_0) - \lambda_{k+1}(A_0) - \sum_{i=1}^K \|B_{0,i}\|_2} \\ &= \frac{\frac{1}{K} \frac{m_0}{m_0+n_0} \sum_{i=1}^K \sin \theta_{0,i}}{1 - \frac{1}{K} \frac{m_0}{m_0+n_0} \sum_{i=1}^K \sin \theta_{0,i}} \end{aligned}$$

□

D. Implementation Details

Robust Loss Functions We conducted experiments with CE, GCE, SCE, ELR mentioned in subsection 3.1. We followed all experiments settings presented in the (Liu et al., 2020) except for the GCE on CIFAR-100 dataset. We used ResNet-34 models for both a proxy model and a target model and trained them using a standard Pytorch SGD optimizer with a momentum of 0.9. We set a batch size of 128 for all experiments. We utilized weight decay of 0.001 and set the initial learning rate as 0.02, and reduce it by a factor of 100 after 40 and 80 epochs for CIFAR-10 and after 80 and 120 epochs for CIFAR-100 except for the GCE on CIFAR-100. For the GCE on CIFAR-100, we set a weight decay lambda as 0.0001, the initial learning rate as 0.01, and reduced it by a factor of 10 after 80 and 120 epochs set in (Zhang & Sabuncu, 2018).

Co-teaching Families As an extension on the original experiments in Co-teaching papers (Han et al., 2018; Yu et al., 2019), we conducted experiments on various noise settings. Because the architecture used in original papers was not trained on the extreme noise setting (e.g. symmetric noise 80%), we used PreAct ResNet-18 models used in (Li et al., 2019) and reported their accuracy.

The performance of such model is quite low when we used the same hyperparameter settings in the Co-teaching+ official code (Yu et al., 2019). Hence, we did preliminary experiments to find the best E_k value in algorithm 3 and algorithm 4 while fixing the other hyperparameter values.

In preliminary experiments, we find the best E_k value as 60 for Co-teaching method when we conducted a grid search on {40, 50, 60, 70}. On the other hand, Co-teaching+ requires larger E_k value because it uses less data than Co-teaching in same iteration. As a result, we found 140 for a E_k value for Co-teaching+ when doing a grid search on {100, 120, 140, 160}.

algorithm 3 and algorithm 4 represent the Co-teaching and Co-teaching+ algorithms, respectively.

Algorithm 3 Co-teaching with our NOISYDETECTOR methods

INPUT : $w^{(1)}, w^{(2)}$: weight parameters for two networks, \mathcal{D} : training set, \mathcal{D}_C : filtered training set, B : batch size , η : learning rate , τ : estimated noise rate, E_k and E_{max} : epoch
 OUTPUT : $w^{(1)}$ and $w^{(2)}$

- 1: **for** $e = 1, \dots, E_{max}$ **do**
- 2: **Shuffle** \mathcal{D} into $\frac{|\mathcal{D}|}{B}$ mini-batches
- 3: **for** $n = 1, \dots, \frac{|\mathcal{D}|}{B}$ **do**
- 4: **Fetch** n -th mini-batch $\bar{\mathcal{D}}$ from \mathcal{D} ;
- 5: **Get** $\bar{\mathcal{D}}^{(1)} = \arg \min_{\mathcal{D}': |\mathcal{D}'| \geq \lambda(e)|\bar{\mathcal{D}}|} \ell(\mathcal{D}'; w^{(1)});$
- 6: **Get** $\bar{\mathcal{D}}^{(2)} = \arg \min_{\mathcal{D}': |\mathcal{D}'| \geq \lambda(e)|\bar{\mathcal{D}}|} \ell(\mathcal{D}'; w^{(2)});$
- 7: **Update** $w^{(1)} = w^{(1)} - \eta \nabla \ell(\bar{\mathcal{D}}^{(2)}; \mathcal{D}_C; w^{(1)});$
- 8: **Update** $w^{(2)} = w^{(2)} - \eta \nabla \ell(\bar{\mathcal{D}}^{(1)}; \mathcal{D}_C; w^{(2)});$
- 9: **end for**
- 10: **Update** $\lambda(e) = 1 - \min\{\frac{e}{E_k} \tau, \tau\}$
- 11: **end for**

DivideMix DivideMix (Li et al., 2019) solves a noisy classification challenge as semi-supervised approach. It trains two separated networks to avoid confirmation errors. The training pipeline consists of *co-divide* phase and semi-supervised learning (SSL) phase. Firstly, in *co-divide* phase, two networks divide the whole training set into clean and noisy subset and provide them to each other. In SSL phase, each network utilizes clean and noisy subset as labeled and unlabeled training set, respectively, and do the MixMatch (Berthelot et al., 2019) after processing label adjustment, *co-refinement* and *co-guessing*. It adjusts the labels of given samples with each model’s prediction, and this adjustment can be thought as a label smoothing for robust training.

In *co-divide* phase, each network calculates cross-entropy (CE) loss value of each training sample and fits them into Gaussian Mixture Model (GMM) with two components which indicate the distribution of clean and noisy subsets. From this process, each sample has clean probability which means how close the sample is to the ‘clean’ components of GMM. However, it is far sensitive to hyperparameter settings because it needs specific threshold to distinguish whether the data is clean or not according to the clean probability of given sample.

Algorithm 4 *Co-teaching+* with our NOISYDETECTOR methods

INPUT : $w^{(1)}, w^{(2)}$: weight parameters for two networks, \mathcal{D} : training set, \mathcal{D}_C : filtered training set, B : batch size, η : learning rate, τ : estimated noise rate, E_k and E_{max} : epoch

OUTPUT : $w^{(1)}$ and $w^{(2)}$

```

1: for  $e = 1, \dots, E_{max}$  do
2:   Shuffle  $\mathcal{D}$  into  $\frac{|\mathcal{D}|}{B}$  mini-batches
3:   for  $n = 1, \dots, \frac{|\mathcal{D}|}{B}$  do
4:     Fetch  $n$ -th mini-batch  $\bar{\mathcal{D}}$  from  $\mathcal{D}$ ;
5:     Select prediction filter and disagreement  $\bar{\mathcal{D}}' \cap \mathcal{D}_C$ ;
6:     Get  $\bar{\mathcal{D}}'^{(1)} = \arg \min_{\mathcal{D}': |\mathcal{D}'| \geq \lambda(e)|\bar{\mathcal{D}}'|} \ell(\mathcal{D}'; w^{(1)});$ 
7:     Get  $\bar{\mathcal{D}}'^{(2)} = \arg \min_{\mathcal{D}': |\mathcal{D}'| \geq \lambda(e)|\bar{\mathcal{D}}'|} \ell(\mathcal{D}'; w^{(2)});$ 
       Update  $w^{(1)} = w^{(1)} - \eta \nabla \ell(\bar{\mathcal{D}}'^{(2)}; w^{(1)});$ 
       Update  $w^{(2)} = w^{(2)} - \eta \nabla \ell(\bar{\mathcal{D}}'^{(1)}; w^{(2)});$ 
8:   end for
9:   Update  $\lambda(e) = 1 - \min\{\frac{e}{E_k} \tau, \tau\}$ 
10: end for

```

We demonstrate that our NOISYDETECTOR methods may be helpful to improve the performance of a given pipeline. As a support, we modify a pipeline by replacing the *co-divide* process with our NOISYDETECTOR methods. In semi-supervised learning scheme, noisy samples can be utilized as unlabeled training set, so TFT which eliminates noisy samples from training set seems not proper in this case. In every training epoch in DivideMix, we get winning tickets with either CLK or SAME for the instances filtered from the *co-divide* process. [algorithm 5](#) represents the details about the modified algorithm, written based on Dividemix original paper. All hyper-parameters settings are same with (Li et al., 2019).

Algorithm 5 *DivideMix* with our NOISYDETECTOR methods

INPUT : $\theta^{(1)}$ and $\theta^{(2)}$: weight parameters of two networks, $\mathcal{D} = (\mathcal{X}, \mathcal{Y})$: training set, τ : clean probability threshold, M : number of augmentations, T : sharpening temperature, λ_u : unsupervised loss weight, α : Beta distribution parameter for MixMatch, NOISYDETECTOR (either CLK or SAME)

OUTPUT : $\theta^{(1)}$ and $\theta^{(2)}$

```

1:  $\theta^{(1)}, \theta^{(2)} = \text{WarmUp}(\mathcal{X}, \mathcal{Y}, \theta^{(1)}, \theta^{(2)})$ 
2: while  $e < \text{MaxEpoch}$  do
3:    $\mathcal{W}^{(2)} = \text{GMM}(\mathcal{X}, \mathcal{Y}, \theta^{(1)})$ 
4:    $\mathcal{W}^{(1)} = \text{GMM}(\mathcal{X}, \mathcal{Y}, \theta^{(2)})$ 
5:    $\mathcal{C}_e^{(2)} = \text{NOISYDETECTOR}(\mathcal{X}, \mathcal{Y}, \theta^{(1)})$ 
6:    $\mathcal{C}_e^{(1)} = \text{NOISYDETECTOR}(\mathcal{X}, \mathcal{Y}, \theta^{(2)})$ 
7:   for  $k = 1, 2$  do
8:      $\mathcal{X}_e^{(k)} = \{(x_i, y_i, w_i) | w_i \geq \tau, (x_i, y_i) \notin \mathcal{C}_e^{(k)}, \forall (x_i, y_i, w_i) \in (\mathcal{X}, \mathcal{Y}, \mathcal{W}^{(k)})\}$ 
9:      $\mathcal{U}_e^{(k)} = \mathcal{D} \setminus \mathcal{X}_e^{(k)}$ 
10:    for  $b = 1$  to  $B$  do
11:      for  $m = 1$  to  $M$  do
12:         $\hat{x}_{b,m} = \text{Augment}(x_b)$ 
13:         $\hat{u}_{b,m} = \text{Augment}(u_b)$ 
14:      end for
15:       $p_b = \frac{1}{M} \sum_m p_{\text{model}}(\hat{x}_{b,m}; \theta^{(k)})$ 
16:       $\bar{y}_b = w_b y_b + (1 - w_b) p_b$ 
17:       $\hat{y}_b = \text{Sharpen}(\bar{y}_b, T)$ 
18:       $\bar{q}_b = \frac{1}{2M} \sum_m (p_{\text{model}}(\hat{u}_{b,m}; \theta^{(1)}) + p_{\text{model}}(\hat{u}_{b,m}; \theta^{(2)}))$ 
19:       $q_b = \text{Sharpen}(\bar{q}_b, T)$ 
20:    end for
21:     $\hat{\mathcal{X}} = \{(\hat{x}_{b,m}, \hat{y}_b); b \in (1, \dots, B), m \in (1, \dots, M)\}$ 
22:     $\hat{\mathcal{U}} = \{(\hat{u}_{b,m}, \hat{y}_b); b \in (1, \dots, B), m \in (1, \dots, M)\}$ 
23:     $\mathcal{L}_{\mathcal{X}}, \mathcal{L}_{\mathcal{U}} = \text{MixMatch}(\hat{\mathcal{X}}, \hat{\mathcal{U}})$ 
24:     $\mathcal{L} = \mathcal{L}_{\mathcal{X}} + \lambda_u \mathcal{L}_{\mathcal{U}} + \lambda_r \mathcal{L}_{\text{reg}}$ 
25:     $\theta^{(k)} = \text{SGD}(\mathcal{L}, \theta^{(k)})$ 
26:  end for
27: end while

```

Winning Ticket in Noisy Image Classification

Datasets (Architecture)	Methods	Symmetric label noise				Asymmetric label noise			
		20%	40%	60%	80%	10%	20%	30%	40%
CIFAR10 (ResNet10)	CCE	89.66	86.62	82.39	68.59	93.96	89.57	85.92	82.41
	GCE	91.47	89.73	86.34	73.91	92.33	88.19	84.93	82.74
	SCE	91.45	89.57	86.27	75.50	91.54	87.44	83.86	80.82
	ELR	92.16	90.49	86.75	69.68	93.21	89.00	85.26	81.73
CIFAR10 (ResNet18)	CCE	91.06	87.91	83.66	72.27	93.07	92.39	91.13	89.19
	GCE	91.77	89.98	86.44	75.50	92.21	91.25	89.95	92.34
	SCE	91.13	88.87	85.15	75.00	91.78	91.35	89.63	85.73
	ELR	92.30	89.13	84.60	70.88	93.80	93.27	92.34	90.24
CIFAR10 (ResNet34)	CCE	91.38	88.43	83.89	70.84	93.54	92.55	91.85	90.05
	GCE	91.34	89.13	85.40	74.75	91.61	91.18	89.22	86.21
	SCE	89.57	86.93	83.38	70.97	91.18	90.14	88.81	85.94
	ELR	91.99	89.71	86.89	72.73	93.11	92.53	91.69	90.28
CIFAR100 (ResNet34)	CCE	64.03	53.24	44.96	23.37	73.66	71.45	66.12	55.72
	GCE	68.92	64.03	54.27	30.78	70.83	68.17	63.01	48.75
	SCE	63.26	53.16	46.33	23.22	71.90	65.65	57.95	49.88
	ELR	74.25	68.05	54.59	26.32	75.16	74.79	74.63	73.73

Table 8. Test accuracies for the models trained with various robust loss function methods on CIFAR-10 and CIFAR-100 dataset.

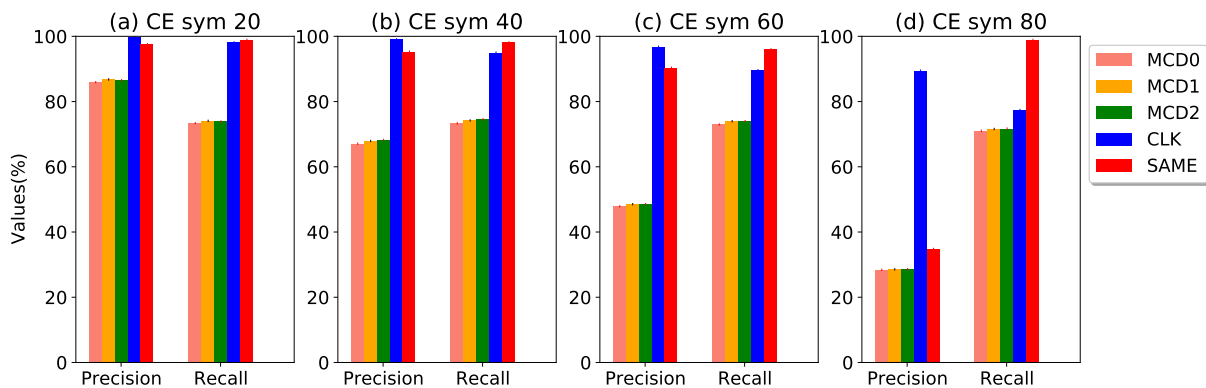


Figure 7. Precision and recall values of the models trained with CE on CIFAR-10. MCD0, MCD1 and MCD2 denotes the output of convolution layer of the last block of ResNet34 respectively.

E. Results

Robust Loss Functions Table 8 provides the test accuracies of various models trained with the robust loss function methods on CIFAR-10 and CIFAR-100 dataset.

Precision and Recall Figure 7 and Figure 8 compare the precision and recall values between Minimum Covariance Determinant (MCD) (Lee et al., 2019), CLK, and SAME methods on CIFAR-10 and CIFAR-100 respectively. MCD0, MCD1 and MCD2 denotes the output of convolution layer of the last block of a ResNet34 model respectively. For calculating the given statistic clean labels are considered as positive class. Thus, precision implies the number of clean samples among selected samples. Recall denotes the number of selected clean samples among all clean samples. As shown in the figures, either CLK or SAME consistently outperforms the MCD method in most cases. Table 9 and Table 10 depicts precision and recall values within various robust loss functions on CIFAR-10 dataset.

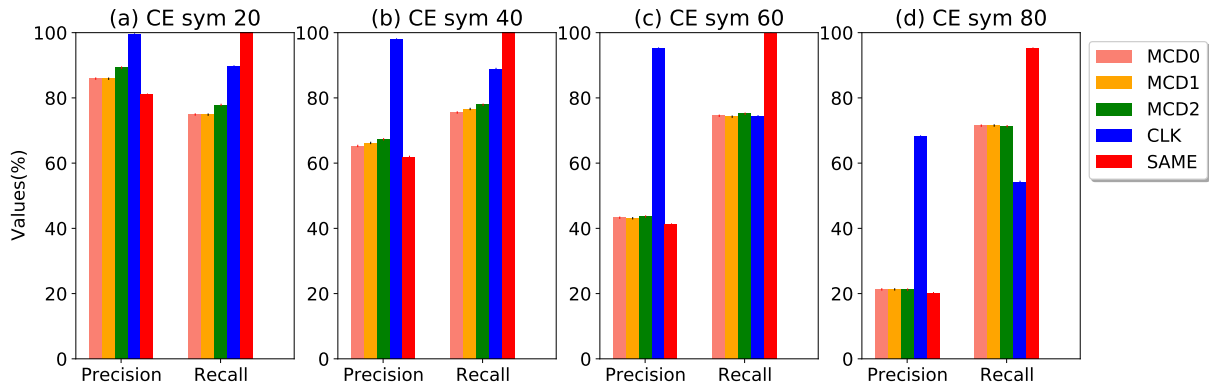


Figure 8. Precision and recall values of the models trained with CE on CIFAR-100. MCD0, MCD1 and MCD2 denotes the output of convolution layer of the last block of ResNet34 respectively.

Appendix References

- Bekker, A. J. and Goldberger, J. Training deep neural-networks based on unreliable labels. In *2016 IEEE International Conference on Acoustics, Speech and Signal Processing (ICASSP)*, pp. 2682–2686. IEEE, 2016.
- Chen, X. and Gupta, A. Weakly supervised learning of convolutional networks. In *Proceedings of the IEEE International Conference on Computer Vision*, pp. 1431–1439, 2015.
- Jindal, I., Nokleby, M., and Chen, X. Learning deep networks from noisy labels with dropout regularization. In *2016 IEEE 16th International Conference on Data Mining (ICDM)*, pp. 967–972. IEEE, 2016.
- Patrini, G., Rozza, A., Krishna Menon, A., Nock, R., and Qu, L. Making deep neural networks robust to label noise: A loss correction approach. In *Proceedings of the IEEE Conference on Computer Vision and Pattern Recognition*, pp. 1944–1952, 2017.
- Sukhbaatar, S., Bruna, J., Paluri, M., Bourdev, L., and Fergus, R. Training convolutional networks with noisy labels. *arXiv preprint arXiv:1406.2080*, 2014.
- Wang, R., Liu, T., and Tao, D. Multiclass learning with partially corrupted labels. *IEEE transactions on neural networks and learning systems*, 29(6):2568–2580, 2017.

Winning Ticket in Noisy Image Classification

Robust Loss	Methods	Symmetric label noise				Asymmetric label noise			
		20%	40%	60%	80%	10%	20%	30%	40%
CE	MCD0	85.95	67.08	47.87	28.37	98.54	95.32	91.26	85.07
	MCD1	86.78	67.90	48.53	28.56	99.43	97.01	92.74	86.51
	MCD2	86.54	68.21	48.54	28.61	99.71	97.07	93.52	87.12
	CLK	99.69	99.04	96.79	89.47	99.65	99.20	98.58	97.99
	SAME	97.57	95.29	90.32	34.79	97.90	95.47	91.40	81.54
GCE	MCD0	87.58	68.68	48.84	28.70	99.45	96.67	92.62	87.74
	MCD1	88.12	69.44	49.17	28.81	99.85	97.46	93.82	89.30
	MCD2	88.23	69.82	49.38	28.90	99.88	97.30	94.44	90.19
	CLK	99.59	98.12	94.54	83.62	99.59	98.86	97.58	93.65
	SAME	99.44	98.26	93.28	55.14	99.65	98.80	95.84	90.06
SCE	MCD0	85.98	67.45	47.75	28.29	97.89	94.77	89.94	84.82
	MCD1	87.83	68.67	47.96	28.50	99.62	96.66	92.20	86.93
	MCD2	86.29	67.44	47.59	28.45	98.86	96.29	93.64	89.21
	CLK	99.64	98.73	96.10	82.98	99.66	99.08	97.99	95.17
	SAME	99.19	98.05	84.91	29.50	99.57	98.55	95.27	90.46
ELR	MCD0	85.73	67.29	47.85	28.54	98.02	96.07	91.72	87.96
	MCD1	86.46	68.09	48.32	28.59	98.41	96.76	93.08	91.03
	MCD2	86.60	67.65	47.86	28.46	98.48	96.93	93.95	92.06
	CLK	99.44	97.46	90.22	57.26	99.46	99.17	98.30	94.29
	SAME	99.68	98.99	97.12	68.92	99.45	99.05	97.97	90.23

Table 9. Precision of ResNet34 models trained with robust loss function on CIFAR-10.

Robust Loss	Methods	Symmetric label noise				Asymmetric label noise			
		20%	40%	60%	80%	10%	20%	30%	40%
CE	MCD0	73.37	73.30	72.96	71.09	72.54	73.79	74.31	73.02
	MCD1	74.08	74.20	73.97	71.58	73.19	75.10	75.52	74.26
	MCD2	73.88	74.54	73.98	71.70	73.40	75.14	76.16	74.78
	CLK	98.11	94.96	89.59	77.42	98.84	97.57	96.37	92.27
	SAME	98.90	98.13	96.01	98.90	99.94	99.93	99.93	99.97
GCE	MCD0	74.76	75.24	74.44	71.93	73.21	74.82	75.42	75.31
	MCD1	75.22	75.87	74.94	92.19	73.51	75.44	76.40	76.65
	MCD2	75.32	76.29	75.27	72.42	73.52	75.32	76.90	77.42
	CLK	97.22	96.31	94.04	85.33	97.39	96.49	95.21	93.54
	SAME	96.81	95.91	94.71	96.02	97.88	97.85	98.34	98.46
SCE	MCD0	73.40	73.70	72.78	70.90	72.06	73.36	73.24	72.80
	MCD1	74.97	75.04	73.10	71.42	73.34	74.82	75.08	74.62
	MCD2	73.66	73.69	72.53	71.29	72.78	74.53	76.25	76.57
	CLK	94.66	92.17	88.79	80.19	95.82	95.10	94.37	92.59
	SAME	95.30	94.06	95.55	96.56	97.83	97.95	98.39	98.44
ELR	MCD0	73.18	73.53	72.93	71.52	72.18	74.36	74.69	75.50
	MCD1	73.82	74.40	73.65	71.66	72.44	74.89	75.79	78.14
	MCD2	73.93	73.92	72.95	71.33	72.50	75.03	76.50	79.02
	CLK	96.48	95.33	93.73	88.96	95.99	96.72	96.42	98.14
	SAME	96.15	94.39	91.50	87.53	97.21	97.84	97.75	99.87

Table 10. Recall of ResNet34 models trained with robust loss function on CIFAR-10.